Microchemical Journal 126 (2016) 322–325

Contents lists available at ScienceDirect

Microchemical Journal

journal homepage: www.elsevier.com/locate/microc

A non-destructive view with X-rays into the strain state of bronze axes☆

L. Glaser [a,*], A. Rothkirch [a], S. Techert [a], M. Freudenberg [b]

[a] Deutsches Elektronen-Synchrotron, Notkestraße 85, D-22607 Hamburg, Germany
[b] Stiftung Schleswig-Holsteinische Landesmuseen Schloss Gottorf, D-24837 Schleswig, Germany

ARTICLE INFO

Article history:
Received 14 July 2015
Received in revised form 2 November 2015
Accepted 2 November 2015
Available online 26 November 2015

Keywords:
Non-destructive
Cultural heritage
Strain analysis
XRD
Bronze
Experimental archeology

ABSTRACT

In this paper we present a new approach using highly surface sensitive X-ray diffraction methods for archaeometrical investigation highlighted on the Neolithic Axe of Ahneby. Applying the $\sin^2\Psi$-method with a scintillation detector and a MAXIM camera setup, both were usually applied for material strain analysis on modern metal fabrics. We can distinguish between different production states of bronze axes: cast, forged and tempered. The method can be applied as a local probe of some 100th of μm^2 or integrative on a square centimeter surface area. We applied established synchrotron radiation based methods of material strain mapping and diffraction on a Neolithic bronze axe as well as replicated material for noninvasive analysis. The main goal of the described investigations was to identify the effects upon the bronze objects of post-cast surface treatment with stone tools and of heat treatment.

© 2015 Published by Elsevier B.V.

1. Introduction

Neolithic and Bronze Age copper and bronze axes are part of our cultural heritage and due to their use as tools, weapons and status symbol good representatives of the state of the art of the ancient metal workers. During the Neolithic time period the previously exclusive stone tools were successively replaced by new materials [1], first copper, then bronze and new methods of production were developed and improved [2]. Being from a time without written documents in northern Europe, objects are the prime source of knowledge with respect to metal working. It is therefore best to carry out investigations in nondestructive ways, keeping the objects preserved for future generations. For a long time, available methods for investigations of the fabric of the objects were limited to sampling and the inspection of polished section. Fortunately that changed and investigation of texture and strain in historic axes was performed using neutron time of flight and neutron diffraction mainly in the last decade [3–6]. Advantages of those methods are the obvious noninvasive approach and the high resolution of phase contrast of the diffraction measurements, as well as bulk sensitivity, which may limit the effects upon the measurement of potential surface corrosion layers. The achievable spatial resolution of neutron investigations is usually limited due to flux and extent of neutron beams (typically in the range of some mm or above). Additionally, bombarding objects with thermal neutrons may radioactively activate the object. We chose an approach which is slightly less accurate concerning the absolute strain measured in the sample, but as we will show in the paper, it helps to easily distinguish the three main states that copper and bronze axes may be in: cast, forged and tempered (after previous cold working). Forging or cold working of bronze leaves visual imprints at the object's surface, which remain unchanged for the eye after tempering. The main advantages using X-rays are the possibility of using any spot size for the measurement from cm^2 down to some 100 μm^2 allowing integrative as well as local measurements, without any chance of activating the specimen chosen or damaging it in any other way. It should be noted that sample penetration depth of X-rays depends on the photon energy applied and in the here presented method is surface sensitive with less than 100 μm penetration depth. For similar applications one should consider that corrosion as patina, surface treatment e.g. with a punch and grain size distribution due to different casting methods may have significant contribution to the measurement. The chosen historic object had the patina completely removed upon finding and the replicated objects were all manufactured identically and cleaned, to investigate the effects of post-cast treatment. The specimens investigated were six replicated objects from the experimental archeological group at Gottorf Palace in well-defined production states using replicated historic tools and an original axe, the Axe of Ahneby (2200–2000 B.C.). The measurements were performed at DESY (Deutsches Elektronen-Synchrotron, Hamburg, Germany) using Beamline G3 [7] at DORIS III.

In the following section the specimen and the experimental setup will be presented.

☆ Selected papers presented at TECHNART 2015 Conference, Catania (Italy), April 27–30, 2015.

* Corresponding author. Tel.: +49 4089985753.
E-mail address: Leif.Glaser@desy.de (L. Glaser).

http://dx.doi.org/10.1016/j.microc.2015.11.004
0026-265X/© 2015 Published by Elsevier B.V.

Fig. 1. The Anglo-Irish Axe from Ahneby, Kreis Schleswig–Flensburg, of the northern Late Neolithic (~2300–1700 B.C.). It is a bronze axe of 25 cm in length and a weight of 700 g. This outstanding object has become so popular that it was integrated in the coat of arms of the parish (top right).

2. Material and methods

The replicas to test the method were produced by the Archaeological State Museum Gottorf Palace (Schleswig, Germany) in cooperation with the Casting Museum Howaldtsche Metallgießerei (Kiel, Germany). Original bronze axes were from the archeological state museum. A special focus was on the effects of potential cold working at the Late Neolithic Axe of Ahneby.

The Axe from Ahneby (Fig. 1), Kreis Schleswig–Flensburg, belongs into the group of so called Anglo-Irish Axes of the northern Late Neolithic. In Schleswig–Holstein this is still a horizon where metal objects are very rare. With a length of 25 cm and a weight of 700 g bronze the axe is an outstanding object, and it had become so popular that it was integrated in the coat of arms of the parish (Fig. 1, top right). As an imported object it might have been made in a different production process as the local products.

The replicas had a bronze stoichiometry of the average of the Axe of Ahneby and were cast using modern techniques. The copper was melted at 1300 °C and then tin was added and mixed for 1–2 min, before the axes were cast in sand cast technique using a foundry ladle. No additives were used for the bronze, except a little carbon to bind the scoria for removal prior to adding tin. Objects were cleaned using brushes and water, while ridges were removed using flint tools. After the first measurements the specimen was cold worked using stone tools, replicated after Neolithic finds [8,9] and tempered in a muffle furnace at 700 °C. This temperature is comparable to a charcoal fire with moderate airflow. After each treatment cycle, strain measurements were carried out and two dimensional X-ray images highlighting grains (or coherent zones) in the sample were taken. The results were compared with measurements performed with the Axe of Ahneby.

For surface sensitive diffraction analysis, two related experiments were performed: one for strain analysis with the $\sin^2\Psi$-method [10–13] using a scintillation detector and one method using the MAXIM camera [7,14] for spatially resolved analysis of the aligned (220) reflexes. The experiments were performed at the G3 beamline (Fig. 2a) with a monochromatic X-ray beam of energy ≈ 6.9 keV. $\mathrm{Sin}^2\Psi$ measurements were carried out by θ–2θ scans at different χ angles in the so called chi-mode (χ equals Ψ here) on the (220) reflection with an incident beam extent of 3 × 3 mm^2. MAXIM images were taken with maximum incident beam extent of about 16 × 6 mm^2 at incidence angle ω of 15° to the sample surface, and thus illuminating a large sample area. Measurements with the MAXIM camera are carried out by illuminating the specimen with a broad (parallel) beam which typically illuminates an area of ~13 mm × 4–13 mm of the specimen (Fig. 3). A signal is measured by a CCD area detector with a multichannnel plate (MCP) in front. The MCP acts as a collimating device for each CCD pixel such, that for a given detector angle e.g. diffraction originating from multiple locations on the sample surface is measured in parallel. MAXIM assembles a silicon chip of total 1024 × 1024 pixel^2 with the pixel size of 13 × 13 μm^2 matching aperture of the MCP. Depending on illumination geometry, the resulting images correspond to an area of ~13 × 13 mm^2 on the sample surface at the best resolution possible. Note that e.g. in case MAXIM collects the signal at an angle off the sample surface normal, projection effects lead to a worse spatial resolution on the sample surface (direction parallel incident beam). In the presented measurements the actual resolution is 13 × 13.2 μm^2 with a specimen sample surface area of 1.7 cm^2 covered.

Analyzing two wide range 2θ scans taken first with the silicon point detector, effects on the different diffraction patterns due to cold working were investigated (Fig. 2b). We observed significant changes in both the (220) and (222) reflexes, while only small changes were found for all other reflexes within the given scan range. The (220) reflex was chosen because of its better angular position close to 90° in particular with respect to MAXIM camera setup constrains, to allow for comparisons/findings from both detectors and due to the increase of intensity upon cold working seen in the data. Diffraction images with the

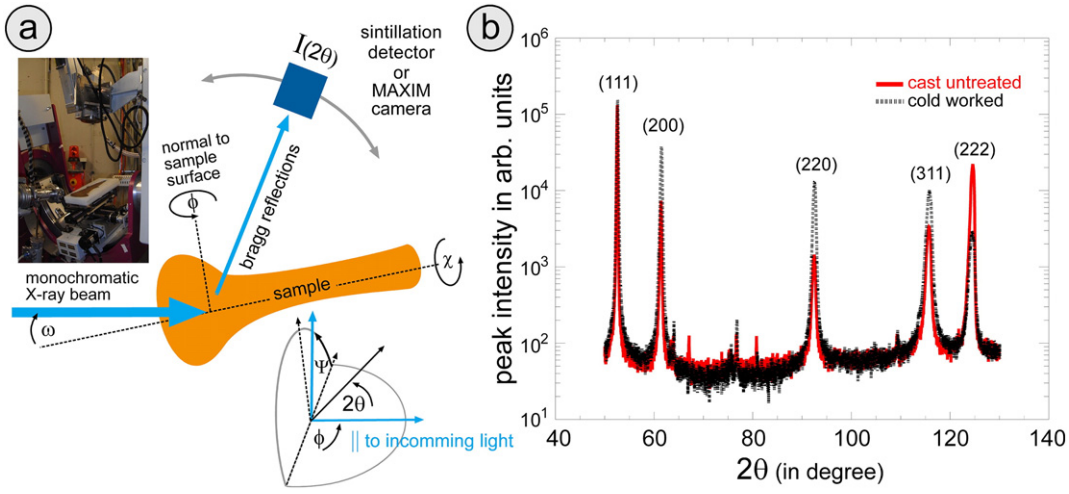

Fig. 2. (a) The experimental setup: The incoming monochromatic X-ray beam along the 2θ = 0° direction hits the bronze axe in gracing incidence. The measurements can be performed using a MAXIM camera or a scintillation detector, which may move along a 2θ circle. When rolling the axe around the beam (χ equals Ψ) the surface stress tensor components $\sigma_{\parallel}$ and $\sigma_{\perp}$ can be measured. (b) The effects of cold working of the bronze can be seen in the peak broadening of all reflexes, but also in the increase of the (220) reflex (at 2θ = 92°) and the decrease of the (222) reflex (at 2θ = 124°) of one order of magnitude each.

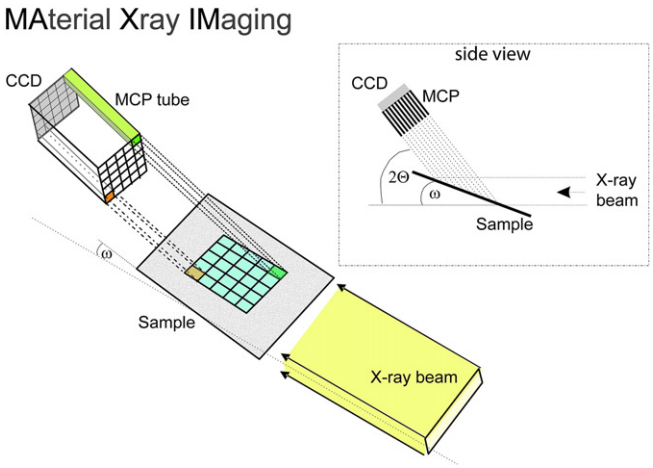

Fig. 3. The MAXIM camera principle: The incoming X-ray beam extends to ~16 × 6 mm² illuminating a sample in gracing incidence at an angle ω. The native resolution of the CCD camera is 13 × 13 μm pixel size, thus with an angle of 2θ differing from ω + 90°, the spatial resolution along the X-ray beam propagation direction decreases, while the pixel elongates with (1/cos) of this angle difference.

MAXIM camera were taken at the (220) reflex distributions as well to allow for the best lateral resolution achievable. For strain measurements with scintillation counter, 24 diffractograms were taken at 6 tilt angles $\chi = [0°, 27°, 39°, 51°, 63°$ and $78°]$ and four 90° Φ rotations around the surface normal of the specimen each. χ being the rotation angle of the ω and 2θ plains normal, with $\chi = 0°$ being the angle the sample surface faces up (as in photograph of Fig. 2a).

This way the two independent components of the stress tensor ($\sigma_{||}$ — along the axe length direction and $\sigma_{\perp}$ — perpendicular to the axe length direction — Fig. 4b middle) could be measured. Data analysis was carried out using IDL [15], as described in the following: For data analysis the measured peaks were fitted to Gaussians with constant background, weighted by the square root of their intensity (Poisson statistics). Standard error propagation was used to account for the error of the mathematical Gaussian fit to the diffraction peak and the position accuracy of the experimental setup.

3. Results and discussion

A wide range 2θ scan (Fig. 2b) of a cast sample and of the same object cold worked shows strong changes in all reflexes but the (111). While the (220) shows an order of magnitude increase in intensity the (222) has an order of magnitude reduced signal upon cold working. Cross checking this result with the area resolving MAXIM camera (Fig. 5a and b) it becomes apparent that the increase and decrease are due to the number of independent grains or small sized groups of in phase grains that contribute to the signal and not by enlarging or shrinking in phase oriented regimes. The (220) reflex was used for all further investigations, showing a diffraction peak at an angle of $2\theta = 92°$ at 6.9 keV photon energy.

A contour plot of the scans taken at the (220) reflex, i.e. plotting the measured intensity color-coded (Fig. 4a) as function of $\sin^2\Psi$ vs. 2θ, shows already that there are strong effects in between cast, tempered and finally forged sample treatment. Comparing the FWHM resulting from Gaussian fits to the different measured peaks, one can evaluate an increase of about 30% from cast peak width (~0.4°) to the forged and tempered states, while there is a factor of 1.5 to 3 in the peak width upon cold working. The cast objects had in some measurements small side peaks at 0.8° to the low angle side, while the tempered objects, if at all, had a small side peak 0.7° to the high angle side in 2θ. Both features show no correlation to either Ψ or Φ on the basis of the available measured sample set at the time. Lattice spacing d was derived from the center position $2\theta_{cen}$ resulting from the Gaussian fits via Braggs Law ($2 \times d \times \sin(\theta) = n \times \lambda$; $\theta = 2\theta_{cen} / 2$) and plotted as normalized displacement from the stress free position d_0, as $(d/d_0) - 1$ vs. $\sin^2\Psi$ (Fig. 4c). The mean of d values obtained for the four datasets taken at $\chi = 0°$ in a scan set was used as substitute for d_0. The slope of the fitted

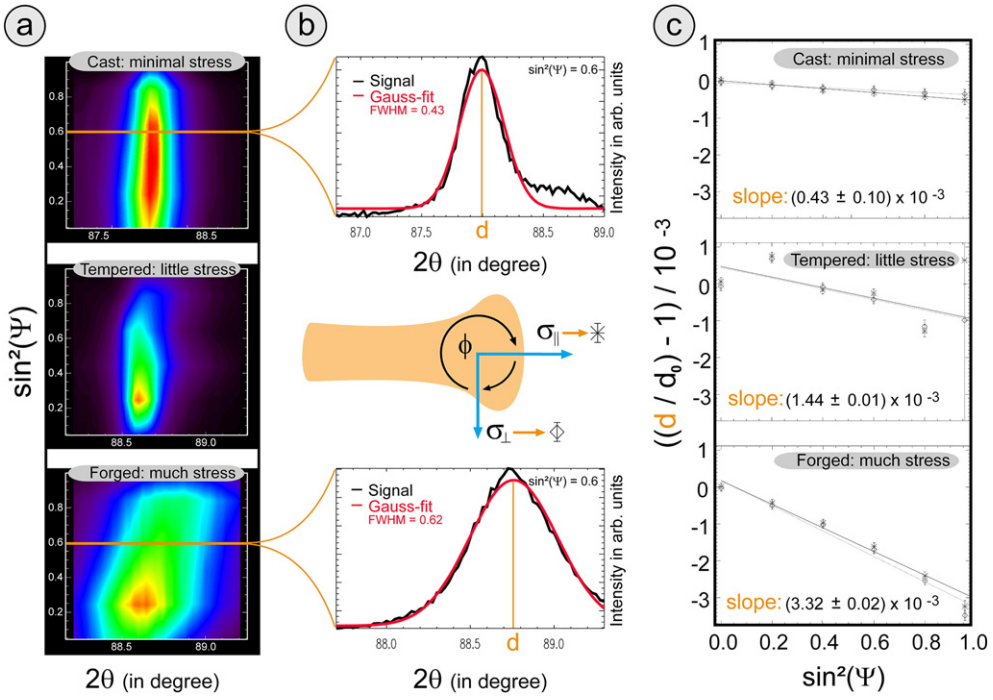

Fig. 4. (a) Contour plots from the scans taken at the (220) reflex as $\sin^2\Psi$ vs. 2θ; a strong effect between cast, forged and tempered and finally forged sample treatment can be seen already. (b) Every 2θ diffractogram is fitted with a Gaussian, which width increases from cast bronze to cold worked bronze by 50%. The lattice spacing d derived from the center position $2\theta_{cen}$ of the Gaussian fits to scans (Ψ, 2θ) was used to obtain a measure for stress by applying the $\sin^2\Psi$-method and the resulting slope value (c). The peak position shifts to higher angles in the presence of surface strain (pressure). The slope of the fitted line through the data points is directly proportional to the surface strain present. The increase from cast to forged is one order of magnitude with these measurements.

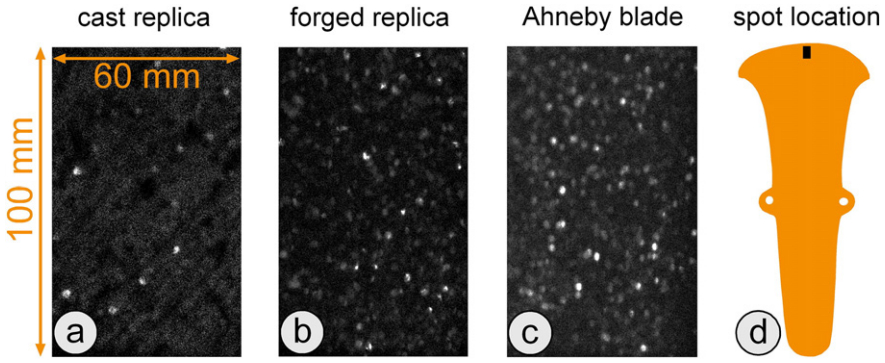

Fig. 5. Using the MAXIM camera the monitored position of in phase oriented (220) reflexes can be displayed as a function of surface treatment. The white spots in the depicted spatial resolved camera pictures represent surface regions of aligned phase orientation, not necessary single grains. A comparison with the blade region of a cast replica (a), a cold worked replica (b) and the Axe of Ahneby (c) leads us to the conclusion that the final treatment of the blade region of the latter one was cold working. The pictures (a) to (c) were all taken on the axes part of the blade as marked in (d) as small black oblong on the axe silhouette.

line through the data points is directly proportional to the surface strain present. As shown in Fig. 4c the increase of stress from simple cast material to finally tempered or finally forged specimen is a factor of 3 and 10 respectively. This allows a distinct identification of the materials to the last surface treatment.

Analyzing the MAXIM pictures was done by normalizing the image intensities to the beamline flux and removing the signal from damaged pixels e.g. bright and dark spots, thus getting similar contrast in all images (as examples displayed in Fig. 5). The cold working of the bronze leads to a significant increase of the phase aligned regions, not necessarily single grains, visual as white spots in the spatially resolved images. This effect was also noted by the increase of the integrated signal of the point detector of an order in magnitude as shown in Fig. 2b. A comparison of the forged replicated material with the original Axe of Ahneby, as shown with MAXIM pictures of the (220) reflex intensity in Fig. 5 for the blade region of the axes, indicates that the final surface treatment procedure of the blade of the Axe of Ahneby was cold working. Measurements far from the blade show no signs of final cold working, comparable with the tempered state of the replicas. The Axe of Ahneby shows visible imprint marks from cold working on the surface of the flanges and the not intensely cleaned areas of the axe surface. We conclude that the axe was at least once cold worked and tempered before the blade was finally hardened by forging.

4. Conclusions

In this paper we demonstrated the usefulness of the $\sin^2\Psi$-method for archaeometric measurements on historic metal objects. The method was successfully applied to distinguish non-destructively between cast, forged and finally tempered regions of bronze objects. Due to the very surface sensitivity of the method applied nothing concerning the effects of forging upon the bulk material of the axes can be concluded, here the application of hard X-rays or neutrons would be suggested. The use of the MAXIM camera gave a more detailed picture, showing the effects of cold working upon the (220) Bragg reflex orientation distribution at the surface. A combination of the two methods applied allowed to clearly identifying that the cold working at the historic Axe of Ahneby has been followed by tempering and finally only the blade region had been cold worked again for the best performance of the axe. This production cycle proven on this 4500 year old axe is still used for good blades even today. The manufacturing technique is quite advanced for such an early time. Much later and half way around the globe the same technique has been brought to perfection by later generations of smiths, leading to the legendary Katana swords of medieval Japan. More systematic investigation on Neolithic material should be performed to identify the origin and the geographical extension of the method. The here demonstrated investigation technique would be a good tool for a non-destructive broad band investigation series of historic objects.

Acknowledgment

The authors like to acknowledge the indispensable help we received with reproducing bronze axes by Armin Leppert and the team at the Howaldtsche Metallgießerei Kiel, as well as the excellent assistance of the Experimental Archaeologist at Gottorf Palace and the splendidly support of Jörn Donges at Beamline G3 at DESY.

References

[1] H. Vandkilde, From stone to bronze, The Metalwork of the Late Neolithic and Earliest Bronze Age in Denmark, Århus1996.
[2] B.R. Armbruster, Goldschmiedekunst und Bronzetechnik, Studien zum Metallhandwerk der Atlantischen Bronzezeit auf der Iberischen Halbinsel, Montagnac, 2000.
[3] R. Arletti, et al., Texture analysis of Bronze Age axes by neutron diffraction, Appl. Phys. A 90 (2008) 9–14.
[4] El'ad N. Caspi, et al., Neutron diffraction study of Levantine Middle Bronze Age cast axes, J. Phys. Conf. Ser. 251 (2010) 012047.
[5] D. Berger, et al., New insights into early Bronze Age damascene technique north of the alps, Antiqu. J. 93 (2013) 25–53.
[6] V. Kiss, et al., Non-destructive analysis of bronze artefacts from Bronze Age Hungary using neutron-based methods, J. Anal. At. Spectrom. 30 (2015) 685–693.
[7] T. Wroblewski, O. Clauß, H.-A. Crostack, A. Ertel, F. Fandrich, Ch. Genzel, K. Hradil, W. Ternes, E. Woldt, A new diffractometer for materials science and imaging at HASYLAB beamline G3, Nucl. Inst. Methods Phys. Res. A 428 (1999) 570–582.
[8] M. Freudenberg, Cushion stones and other stone tools for early metalworking in Schleswig–Holstein. Some new aspects on local Bronze Age Society, in: F.B.L. Astruc, V. Lea, P.-Y. Milcent, S. Philibert (Eds.),Normes techniques et pratiques sociales: de la simplicité des outillages pré- et protohistoriques, Antibes 2006, pp. 313–320.
[9] M. Freudenberg, Steingeräte zur Metallbearbeitung - Einige neue Aspekte zum spätneolithischen und frühbronzezeitlichen Metallhandwerk vor dem Hintergrund des schleswig-holsteinischen, Fundmaterials Archäologisches Korrespondenzblatt 39 (2009) 341–359.
[10] Eckard Macherauch, Paul Muller, Das $\sin^2\psi$-Verfahren der rontgenographischen Spannungsmessung, Z. Angew. Phys. 13 (1961) 305–312.
[11] I.C. Noyan, J.B. Cohen, Residual Stress — Measurements by Diffraction and Interpretation, Springer-Verlag, New York, USA, 1987.
[12] Viktor Hauk (Ed.), Structural and Residual Stress Analysis by Nondestructive Methods, Elsevier Science B.V., Amsterdam, The Netherlands, 1997.
[13] Lothar Spies, Robert Schwarzer, Herfried Behnken, Gerd Teichert, Moderne Röntgenbeugung - Röntgendiffraktometrie für Materialwissenschaftler, Physiker und Chemiker, 1st edition B.G. Teubner Verlag/GWV Fachverlage GmbH, Wiesbaden, Germany, 2005.
[14] André Rothkirch, Sabiene Lenser, Imaging diffraction using Maxim at G3/HASYLAB — spatial resolved strain measurements on linear friction welded dissimilar materials, Mater. Sci. Forum 571–572 (2008) 237–242.
[15] http://www.exelisvis.com/ProductsServices/IDL.aspx (last accessed 2015/10/30).